

Medium permittivity bismuth zinc niobate thin film capacitors

R. L. Thayer, C. A. Randall, and S. Trolier-McKinstry^{a)}

Center for Dielectric Studies, Materials Research Institute, The Pennsylvania State University, University Park, Pennsylvania 16802

(Received 14 February 2003; accepted 19 May 2003)

Thin films were fabricated via metalorganic decomposition methods with three compositions: $\text{Bi}_{1.5}\text{Zn}_{1.0}\text{Nb}_{1.5}\text{O}_7$, $\text{Bi}_{1.5}\text{Zn}_{0.5}\text{Nb}_{1.5}\text{O}_{6.5}$, and $\text{Bi}_2\text{Zn}_{2/3}\text{Nb}_{4/3}\text{O}_7$. The $\text{Bi}_{1.5}\text{Zn}_{0.5}\text{Nb}_{1.5}\text{O}_{6.5}$ composition is a low temperature phase with the cubic pyrochlore structure. This phase may undergo a peritectoid decomposition at 700°C to the high temperature phases of $\text{Bi}_{1.5}\text{Zn}_{1.0}\text{Nb}_{1.5}\text{O}_7$ and BiNbO_4 . Both the $\text{Bi}_{1.5}\text{Zn}_{1.0}\text{Nb}_{1.5}\text{O}_7$ and $\text{Bi}_{1.5}\text{Zn}_{0.5}\text{Nb}_{1.5}\text{O}_{6.5}$ cubic pyrochlores show medium room temperature permittivities (150 and 180, respectively) with negative temperature coefficients of capacitance and a low temperature dielectric relaxation. Both $\text{Bi}_{1.5}\text{Zn}_{1.0}\text{Nb}_{1.5}\text{O}_7$ and $\text{Bi}_{1.5}\text{Zn}_{0.5}\text{Nb}_{1.5}\text{O}_{6.5}$ films showed substantial dielectric tunability with electric field ($>30\%$). The field dependence of the dielectric permittivity of the zirconolite structured $\text{Bi}_2\text{Zn}_{2/3}\text{Nb}_{4/3}\text{O}_7$ thin films demonstrates an unusual field induced transition at high field $\sim 2\text{ MV/cm}$, with a maximum tunability of 20%. It is hypothesized that this is associated with field forced ordering of the Zn atoms between two closely spaced, partially occupied sites. © 2003 American Institute of Physics. [DOI: 10.1063/1.1590415]

I. INTRODUCTION

In thin films, as in bulk dielectrics, there is a need to develop materials that are medium to high permittivity ϵ_r , but with low temperature coefficients of capacitance (TCC's) and low dielectric loss values. Such materials would be important for integrated passive components, such as resistor-capacitor arrays, for on-chip applications including integrated decoupling capacitors, and in microwave applications. In all cases, low processing temperatures are desired. If the material also has a field-tunable permittivity, then it should be possible to actively tune the circuit.

Several materials have been considered for these applications. Considering only materials with a permittivity in excess of 20, the following information is available in the literature. Nakagawara *et al.* demonstrated that $(\text{Zr},\text{Sn})\text{TiO}_4$ films could be prepared with $\epsilon_r=38$ and $\text{TCC}=20\text{ ppm}/^\circ\text{C}$ and low dispersion in the properties out to the microwave frequency range.¹ $\text{Ba}(\text{Mg}_{1/3}\text{Ta}_{2/3})\text{O}_3$ films were shown to have $\epsilon_r=22.2$, $\tan\delta\sim 0.009$, and $\text{TCC}=-145\text{ ppm}/^\circ\text{C}$, with negligible bias dependence of the permittivity.² Modified Ta_2O_5 films have also been shown to have permittivities in the range of 20–43 for $\text{TCC}=11-14\text{ ppm}/^\circ\text{C}$.³⁻⁵ Klee and co-workers⁵ demonstrated that BiNbO_4 films doped with vanadium or copper oxides showed $\epsilon_r=50-58$, $\tan\delta\sim 0.003-0.03$, and TCC's within the range of $\pm 60\text{ ppm}/^\circ\text{C}$. Paraelectric and ferroelectric compositions typically show much larger temperature coefficients, unless the film preparation method results in unusually low permittivities.^{5,6} Ren *et al.* described the family of bismuth zinc niobate (BZN) thin films, with compositions of $\text{Bi}_{1.5}\text{Zn}_{1.0}\text{Nb}_{1.5}\text{O}_7$ and $\text{Bi}_2\text{Zn}_{2/3}\text{Nb}_{4/3}\text{O}_7$. It was shown that these films have permittivities in the range of 80–150, $\tan\delta<0.005$ with modest

TCC's ($+150$ to $-400\text{ ppm}/^\circ\text{C}$) which can be tuned to near zero either by modulating the processing temperature or by making a phase mixture of the two end members.⁷ Epitaxial films of $(\text{Ca}_{1-x}\text{Sr}_x)\text{Bi}_4\text{Ti}_4\text{O}_{15}$ have also been shown to have permittivities of ~ 200 and TCC's varying from -147 to $+88\text{ ppm}/^\circ\text{C}$.⁸ Of these reports, the family of bismuth-based pyrochlores offers a combination of comparatively high permittivities, coupled with tailorable TCC's and the possibility of low processing temperatures.

The general cubic pyrochlore formula is $A_2B_2O_6O'$; it is considered to be a derivative of the fluorite structure AO_2 , where the unit cell is doubled in all dimensions and the A site is split into both A and B sites. The larger A cations are eightfold coordinated with oxygen, yielding distorted cubes. The smaller B cations are sixfold coordinated with oxygen, yielding distorted octahedra. One of the seven oxygens is bonded only to A cations.^{9,10} Based on the refinement of the crystal structure of bulk bismuth zinc niobates, there are two main phases of interest for high frequency dielectrics: a cubic pyrochlore phase with space group $Fd\bar{3}m$ [shown in Fig. 1(a) for $\text{Bi}_{1.5}\text{Zn}_{0.96}\text{Nb}_{1.5}\text{O}_{6.92}$] and a monoclinic zirconolite phase with space group $C2/c$, which has been described as a derivative of the pyrochlore structure [Fig. 1(b)].¹¹ According to structural refinements using neutron diffraction data from monoclinic $\text{Bi}_2\text{Zn}_{2/3}\text{Nb}_{4/3}\text{O}_7$, Nb preferentially occupies sixfold coordinated sites in octahedral sheets parallel to the (001) planes, while Zn is distributed between two fivefold coordinated sites near the centers of the six-membered rings of $[\text{Nb}(\text{Zn})\text{O}_6]$ octahedral layers. The Nb/Zn cation layers alternate along the c axis with Bi layers.¹²

The bulk Bi pyrochlores have a low sintering temperature, below 950°C .^{13,14} $\text{Bi}_{1.5}\text{Zn}_{1.0}\text{Nb}_{1.5}\text{O}_7$ has a permittivity of 150 and TCC of $\sim -400\text{ ppm}/^\circ\text{C}$, while $\text{Bi}_2\text{Zn}_{2/3}\text{Nb}_{4/3}\text{O}_7$ has a permittivity of 80 and TCC of $200\text{ ppm}/^\circ\text{C}$. Additionally, bulk $\text{Bi}_{1.5}\text{Zn}_{1.0}\text{Nb}_{1.5}\text{O}_7$ shows a low temperature dielec-

^{a)}Electronic mail: stmckinstry@psu.edu

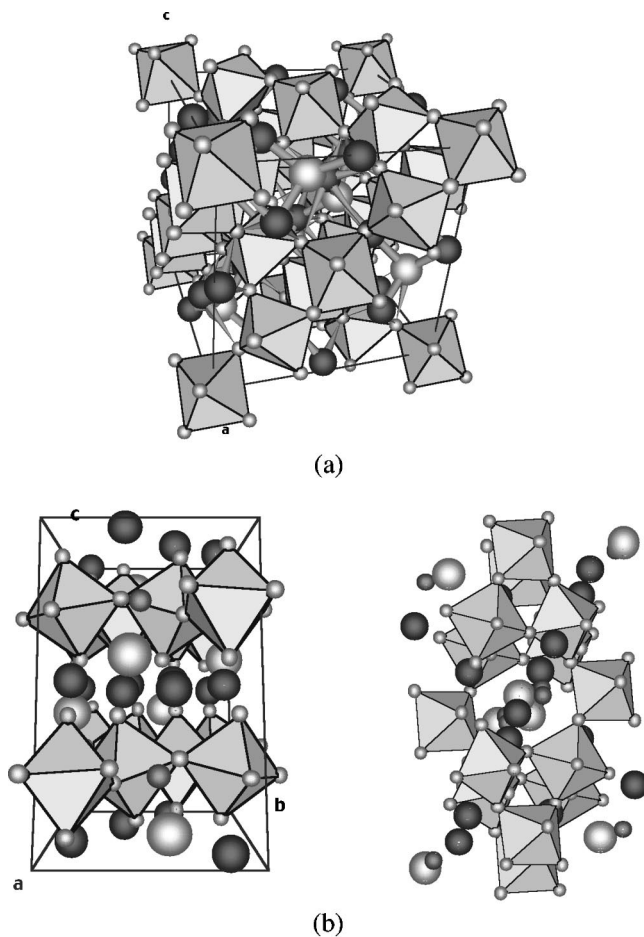


FIG. 1. (a) Schematic structure of the cubic pyrochlore and (b) zirconolite structure. The zinc/niobium centered oxygen octahedra are shown. Bi is the larger dark atom; O is shown as white; Zn is the smaller gray atom in (b).

tric relaxation. Kamba *et al.* studied this dielectric relaxation from 10 to 400 K, and in the frequency range from 100 Hz to 100 THz.^{15,16} From the dielectric dispersion data, the distribution functions of the relaxation frequencies were modeled. Over this temperature range, the relaxation, as assessed from the maximum in $\tan \delta$, follows the Arrhenius law,

$$\nu = \nu_0 \exp(-E_a/k_B T), \quad (1)$$

where ν is the characteristic relaxation frequency, ν_0 is the attempt jump frequency, E_a is the activation energy, and k_B is the Boltzmann constant, with $\nu_0 = 6.13 \times 10^{12}$ Hz and $E_a = 0.202$ eV.

Unlike most ferroelectric thin films, it was found that the dielectric properties of BZN thin films on the order of 0.3 μm in thickness are comparable to those reported for bulk BZN.^{7,17} The similarity between the values for bulk and thin film BZN contrasts to that normally observed in ferroelectrics such as $\text{Ba}_{0.7}\text{Sr}_{0.3}\text{TiO}_3$, in which thin films tend to have severely suppressed permittivities compared to bulk specimens.¹⁸ The objective of this paper is to further investigate the phase formation of the BZN materials and to characterize the field dependence of the dielectric permittivities in thin film form.

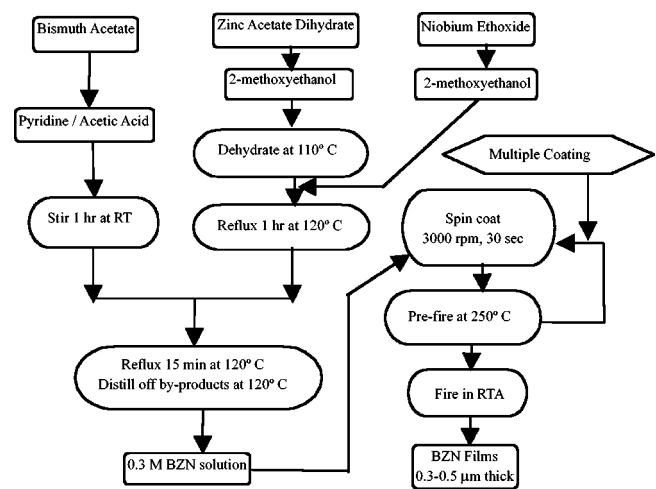


FIG. 2. MOD processing route for the BZN films.

II. EXPERIMENTAL PROCEDURE

Three compositions of BZN thin films: $\text{Bi}_{1.5}\text{Zn}_{1.0}\text{Nb}_{1.5}\text{O}_7$, $\text{Bi}_{1.5}\text{Zn}_{0.5}\text{Nb}_{1.5}\text{O}_{6.5}$, and $\text{Bi}_2\text{Zn}_{2/3}\text{Nb}_{4/3}\text{O}_7$, were prepared by metalorganic decomposition (MOD) on platinumized silicon wafers. The solution was prepared in a manner similar to that previously reported for BZN films.⁷ The precursors used were bismuth acetate, zinc acetate dihydrate (Aldrich Chemical Company, Inc., Milwaukee, WI), and niobium ethoxide (Chemat Technology, Inc., Northridge, CA). The solvents used were 2-methoxyethanol (2-MOE), pyridine, and glacial acetic acid (Aldrich). Zinc acetate dihydrate and 2-MOE were combined, then heated to 120°C, and vacuum distilled in a rotary evaporator in order to remove any water. Niobium ethoxide was mixed with 2-MOE and then added to the zinc solution and refluxed under argon at 120°C for 1 h and then vacuum distilled to remove by-products. Bismuth oxide was introduced into the system by first combining bismuth acetate and pyridine and stirring for 5 min. Glacial acetic acid (30 vol %) was added, and the solution was stirred for 0.5 h until it became clear. This bismuth solution was then added and refluxed under argon at 120°C for 15 min. Finally, the solution was vacuum distilled; then 2-MOE was added to the (Zn,Nb) solution until a concentration of 0.3M was obtained. To prepare thin films, the precursor solution was spin coated at 3000 rpm for 30 s on Pt-coated Si wafers Pt(175nm)/Ti(20nm)/SiO₂(500nm)/Si (Ramtron International Corp., Colorado Springs, CO). The substrate was then placed on a hotplate at 350°C for 1 min to remove organics from the film. This procedure was repeated to build up the film thickness, typically to a thickness of 0.3–0.4 μm , after 3–4 layers were deposited. A rapid thermal annealer was used to crystallize the films, with a heating rate of 100°C/min and a soak time of 120 s in flowing air. Figure 2 summarizes the basic processing route for the MOD films fabricated in this study.

In order to measure electrical properties, an array of Pt dots ranging from 0.5 to 1.15 mm in diameter were sputtered onto the films through a shadow mask to form the top electrodes in a Pt/BZN/Pt configuration. The films were then annealed 50–100°C below their crystallization temperature

for 45–60 s to improve the Pt/BZN interface of the top electrode. If a much lower temperature or a shorter anneal was used, the value of the loss tangent was higher, while higher temperatures and longer times did not affect the loss tangent. The areas of the top electrodes were measured using an optical microscope. To gain access to the bottom electrode, a corner of each film was etched with a 15% HF solution until the bottom Pt layer was exposed, then rinsed with ethanol. After etching, the film thickness was measured by an Alpha-Step 500 surface profiler (Tencor, Portsmouth, NH).

The crystallinity and phase content of the films were characterized with a Scintag DMC-105 x-ray diffractometer (Scintag, Inc., Sunnyvale, CA) using Cu $K\alpha$ radiation at a scan rate of $1^\circ 2\theta/\text{min}$.

The low field dielectric properties of the BZN films were measured with a Hewlett-Packard 4192A LF Impedance Analyzer (Agilent Technologies, Inc., Palo Alto, CA) with an ac oscillation voltage of 0.03 V rms over the frequency range 1–100 kHz. Temperature coefficient of capacitance measurements utilized the HP 4274A Multi-Frequency LCR Meter (Agilent). The temperature was controlled using a Delta Design 2300 oven (Delta Design, Inc., Poway, CA). During these TCC measurements, the samples were heated to 120°C (to remove moisture from the chamber) and the capacitance and loss were measured on cooling to $\sim -50^\circ\text{C}$. The samples were measured using a sample holder that connected to the LCR meter through the oven door. The sample itself was contacted using probe tips on the end of wires that could be bent to change the position of the probe in order to measure a number of electrodes; also, the wires could be bent to adjust the pressure on the electrodes to ensure a good contact.

The low temperature permittivity and loss measurements utilized the HP 4284A Precision LCR Meter (Agilent) over the frequency range 100 Hz to 100 kHz. The low temperature was reached by cooling the sample at approximately $2^\circ\text{C}/\text{min}$ in a Dewar filled with helium.

The high dc field measurements were made using the HP 4274A Multi-Frequency LCR Meter, and a Keithley Instruments 240A high voltage supply (Keithley Instruments, Inc., Cleveland, OH). With an oscillation voltage of 0.03 V, a dc voltage sweep was made starting at 0 V, increasing to the maximum positive dc voltage, decreasing to the maximum negative dc voltage, and returning to 0. These measurements were made at room temperature, 77 K (using liquid nitrogen), and intermediate temperatures using the Delta Design oven.

III. RESULTS AND DISCUSSION

A. Crystallization and phases

Guided by earlier investigations on $\text{Bi}_2\text{O}_3\text{-ZnO-Nb}_2\text{O}_5$, compositions of $\text{Bi}_{1.5}\text{Zn}_{1.0}\text{Nb}_{1.5}\text{O}_7$ and $\text{Bi}_2\text{Zn}_{2/3}\text{Nb}_{4/3}\text{O}_7$ were selected.^{7,9,10,13,14,19–21} During this investigation, a phase based on the composition $\text{Bi}_{1.5}\text{Zn}_{0.5}\text{Nb}_{1.5}\text{O}_{6.5}$ was discovered via the MOD route. This composition was pursued in an attempt to make a sample with no Zn on the A site. It should be pointed out that in the solid state calcination route, this phase could not be formed at the higher temperatures re-

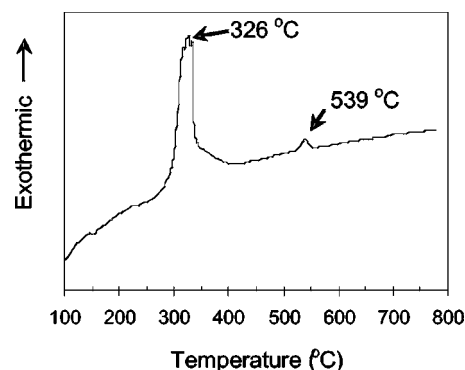


FIG. 3. DTA curve of $\text{Bi}_{1.5}\text{Zn}_{0.5}\text{Nb}_{1.5}\text{O}_{6.5}$ MOD solution.

quired for the interdiffusion of the reactants between particulate precursors.¹⁴ Differential thermal analysis (DTA) was then performed on a BZN gel, which was formed by heating a MOD solution to 120°C to remove liquid organics. A typical DTA curve is observed in Fig. 3. The exothermic peak at 360°C corresponds to the decomposition of the remaining organics. The second exothermic peak at 540°C corresponds to crystallization of the BZN. These DTA data are qualitatively very similar to the earlier studies of $\text{Bi}_{1.5}\text{Zn}_{1.0}\text{Nb}_{1.5}\text{O}_7$ and $\text{Bi}_2\text{Zn}_{2/3}\text{Nb}_{4/3}\text{O}_7$ by Ren *et al.*⁷ Figure 4 shows the x-ray diffraction patterns of $\text{Bi}_{1.5}\text{Zn}_{0.5}\text{Nb}_{1.5}\text{O}_{6.5}$ films following various heat treatments between 500 and 700°C . The x-ray data are in good agreement with the DTA data, that is there is no evidence for crystallization until a temperature of 550°C . On analysis of the diffraction peaks, the structure is consistent with a cubic pyrochlore through crystallization temperatures up to 650°C . When fired at 700°C , the film decomposes into two phases: BiNbO_4 and the cubic pyrochlore $\text{Bi}_{1.5}\text{Zn}_{1.0}\text{Nb}_{1.5}\text{O}_7$. This is consistent with the high temperature phase equilibria determined by solid state calcination studies, which suggest that the low zinc content phase is not stable at elevated temperatures. One possible explanation of these data is that the $\text{Bi}_{1.5}\text{Zn}_{0.5}\text{Nb}_{1.5}\text{O}_{6.5}$ phase is a low temperature phase that undergoes a peritectoid decomposition at approximately 700°C . A summary of the phase development in the three different compositions is given in Table I.

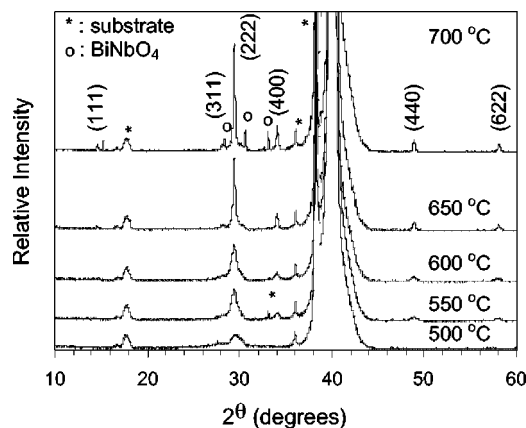


FIG. 4. X-ray diffraction patterns of $\text{Bi}_{1.5}\text{Zn}_{0.5}\text{Nb}_{1.5}\text{O}_{6.5}$ films fired at different temperatures.

TABLE I. Phase development in BZN films.

	$\text{Bi}_2\text{Zn}_{2/3}\text{Nb}_{4/3}\text{O}_7$	$\text{Bi}_{1.5}\text{Zn}_{1.0}\text{Nb}_{1.5}\text{O}_7$	$\text{Bi}_{1.5}\text{Zn}_{0.5}\text{Nb}_{1.5}\text{O}_{6.5}$
550 °C	Cubic	Cubic	Cubic
600 °C	Cubic	Cubic	Cubic
650 °C	Cubic	Cubic	Cubic
700 °C	Mixed	Cubic	Decomposes (BiNbO_4
750 °C	Monoclinic	Cubic	and cubic pyrochlore)

B. Low field dielectric properties

Figure 5 shows the room temperature relative permittivity and loss tangent (at 10 kHz) of BZN thin films as a function of firing temperature; the data for $\text{Bi}_{1.5}\text{Zn}_{1.0}\text{Nb}_{1.5}\text{O}_7$ and $\text{Bi}_2\text{Zn}_{2/3}\text{Nb}_{4/3}\text{O}_7$ agree well with those reported earlier.⁷ The permittivity of $\text{Bi}_{1.5}\text{Zn}_{0.5}\text{Nb}_{1.5}\text{O}_{6.5}$ increased with increasing firing temperature, reaching a maximum room temperature permittivity value of 180 at 10 kHz for films fired at 600–650 °C. The higher permittivity observed in this composition suggests that the film is indeed a previously unknown compound. At 700 °C, the permittivity falls, as is to be expected given the decomposition to a lower permittivity Bi pyrochlore with stoichiometry $\text{Bi}_{1.5}\text{Zn}_{1.0}\text{Nb}_{1.5}\text{O}_7$ and low permittivity BiNbO_4 ($\epsilon \sim 42$). The dielectric loss is low for all of the crystallization temperatures ($\tan \delta \sim 0.005$). For compounds for which bulk permittivity data are available, the relative permittivities of BZN films are quite close to those shown in bulk ceramics. This is often not the case with ferroelectric or paraelectric films, where in plane stress clamps polarizability and low permittivity interfacial layers strongly dilute the dielectric response.¹⁸

The TCC's are compared for each composition against firing temperatures between 550 and 750 °C in Fig. 6. Extremely low TCC's can be designed into these medium permittivity dielectrics. It is especially interesting that the $\text{Bi}_{1.5}\text{Zn}_{0.5}\text{Nb}_{1.5}\text{O}_{6.5}$ phase shows both a higher permittivity (180) and a lower TCC (-230 ppm/°C), while requiring a 150 °C lower processing temperature than $\text{Bi}_{1.5}\text{Zn}_{1.0}\text{Nb}_{1.5}\text{O}_7$. This combination should be especially attractive for integrated capacitor applications.

Figure 7 compares the temperature dependence of the permittivity and dielectric loss for the two cubic pyrochlores $\text{Bi}_{1.5}\text{Zn}_{1.0}\text{Nb}_{1.5}\text{O}_7$ and $\text{Bi}_{1.5}\text{Zn}_{0.5}\text{Nb}_{1.5}\text{O}_{6.5}$. A similar dielec-

tric relaxation is observed in both materials; however, the relative permittivity of $\text{Bi}_{1.5}\text{Zn}_{0.5}\text{Nb}_{1.5}\text{O}_{6.5}$ is higher at room temperature and the drop associated with the relaxation is approximately 50 °C lower than in $\text{Bi}_{1.5}\text{Zn}_{1.0}\text{Nb}_{1.5}\text{O}_7$ at a given frequency. This has the attractive properties of higher permittivity at higher temperatures and also a low dielectric loss for a given frequency at room temperature and above. It should also extend the available high frequency range at which these films will have reasonable Q values. The maximum in the dielectric loss data can be used to describe the relaxation behavior, as with earlier studies on the bulk materials. An Arrhenius equation [Eq. (1)] was used to describe the thermally activated process underlying the relaxation for $\text{Bi}_{1.5}\text{Zn}_{0.5}\text{Nb}_{1.5}\text{O}_{6.5}$ (see Fig. 8). The $\text{Bi}_{1.5}\text{Zn}_{0.5}\text{Nb}_{1.5}\text{O}_{6.5}$ film has an activation energy $E_a \sim 0.11 \pm 0.0054$ eV and preexponential jump frequency $\nu_0 \sim 4.57(\pm 2.86) \times 10^{12}$ Hz. These values are similar to those reported earlier in thin film and in bulk BZN ceramics.^{15,16}

C. Electric-field strength dependence of the permittivity

The high field tunabilities of $\text{Bi}_{1.5}\text{Zn}_{1.0}\text{Nb}_{1.5}\text{O}_7$, $\text{Bi}_{1.5}\text{Zn}_{0.5}\text{Nb}_{1.5}\text{O}_{6.5}$, and $\text{Bi}_2\text{Zn}_{2/3}\text{Nb}_{4/3}\text{O}_7$ were all investigated using a small signal ac field over a dc bias. $\text{Bi}_{1.5}\text{Zn}_{1.0}\text{Nb}_{1.5}\text{O}_7$ has previously been reported to have a modest tunability of $\sim 10\%$ for applied biases of ± 830 kV/cm.⁷ It was found here that with increasing bias field the available tunability could be increased substantially at room temperature (see Fig. 9). Throughout the measurement, the dielectric loss of the sample remains low and no hysteresis was observed on retracing the curves.

To investigate the maximum tunability that can be achieved, measurements were repeated at 77 K. Low temperatures were selected to decrease the electronic conductivity, thereby enabling higher fields to be applied without di-

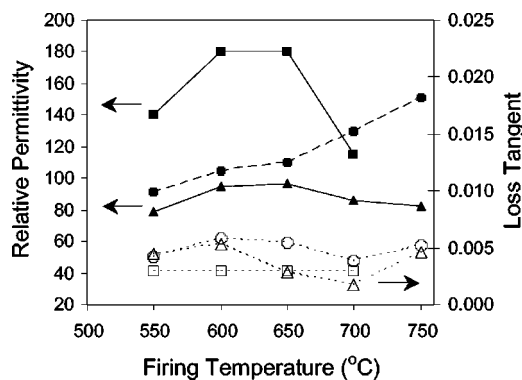


FIG. 5. Relative permittivity and loss tangent of BZN films at different firing temperatures, measured at 10 kHz and 0.03 V ac.

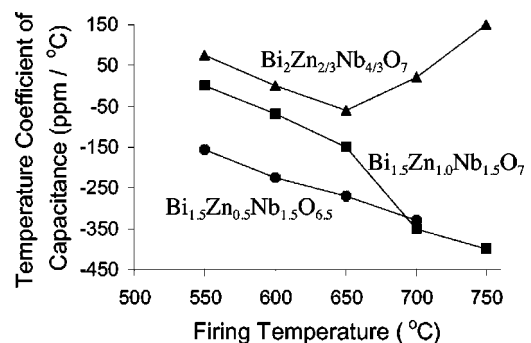


FIG. 6. TCC of BZN films at different firing temperatures.

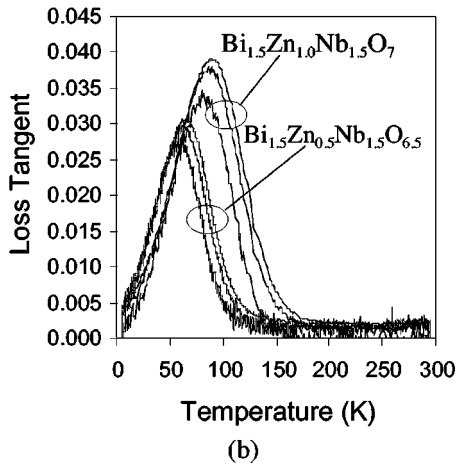
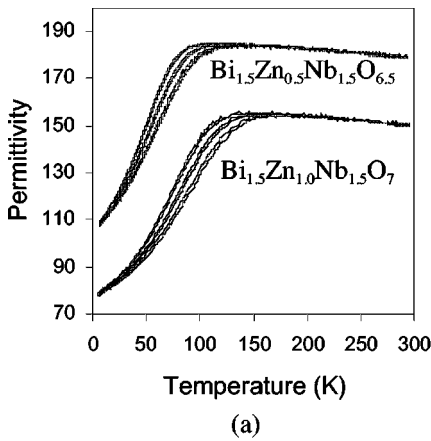


FIG. 7. (a) Permittivity and (b) loss of $\text{Bi}_{1.5}\text{Zn}_{0.5}\text{Nb}_{1.5}\text{O}_{6.5}$ films (fired at 600°C) and $\text{Bi}_{1.5}\text{Zn}_{1.0}\text{Nb}_{1.5}\text{O}_7$ films (fired at 750°C) as a function of measuring temperature. For each composition, the frequency increases from the top curve to the bottom curve in the order 0.5, 1, 5, 10, 50, 100 kHz for permittivity and 10, 5, 1 kHz for the loss tangent.

electric breakdown. Figure 10 shows the permittivity and loss at a temperature of 77 K as a function of applied dc bias for $\text{Bi}_{1.5}\text{Zn}_{1.0}\text{Nb}_{1.5}\text{O}_7$, $\text{Bi}_{1.5}\text{Zn}_{0.5}\text{Nb}_{1.5}\text{O}_{6.5}$, and $\text{Bi}_2\text{Zn}_{2/3}\text{Nb}_{4/3}\text{O}_7$. Again, no hysteresis was observed, since the data from each cycle can be superimposed. The shape of the curves for the field dependence of the permittivity for the two cubic pyrochlore compositions is similar. Both show a gradual reduction with increasing field strength. No defini-

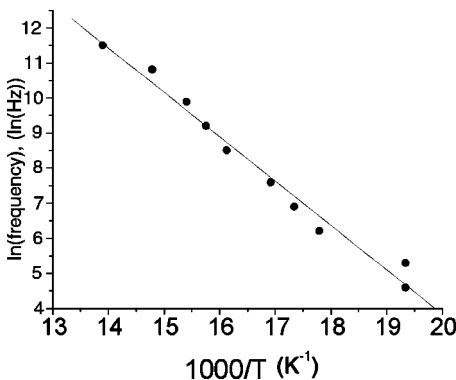


FIG. 8. Arrhenius plot of $\text{Bi}_{1.5}\text{Zn}_{0.5}\text{Nb}_{1.5}\text{O}_{6.5}$ based on curve-fit data in Fig. 7(b).

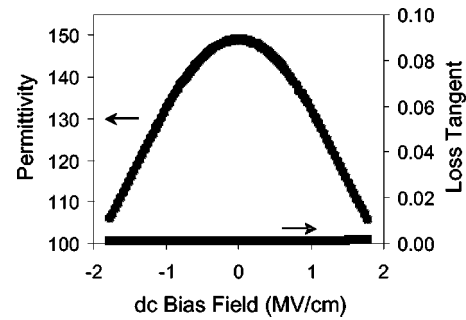


FIG. 9. Permittivity and loss tangent of $\text{Bi}_{1.5}\text{Zn}_{1.0}\text{Nb}_{1.5}\text{O}_7$ as a function of applied dc field, measured at 10 kHz and 0.03 V ac at room temperature.

tive saturation of the permittivity was achieved for the field range utilized. Up to 46% tunability was obtained in $\text{Bi}_{1.5}\text{Zn}_{1.0}\text{Nb}_{1.5}\text{O}_7$. The resulting curve could be fitted well to a sixth order polynomial containing only even terms in the field. It was also found that the fractional tunability was the same at room temperature and at 77 K, even though this entailed measurements both within and well above the relaxation region. The resulting temperature stability should be useful in designing temperature stable tunable components

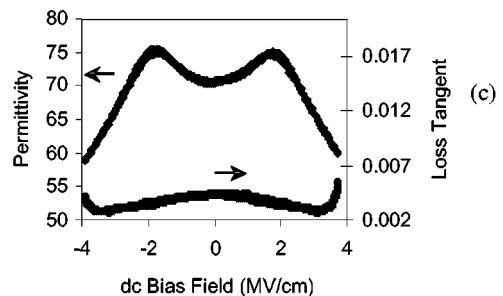
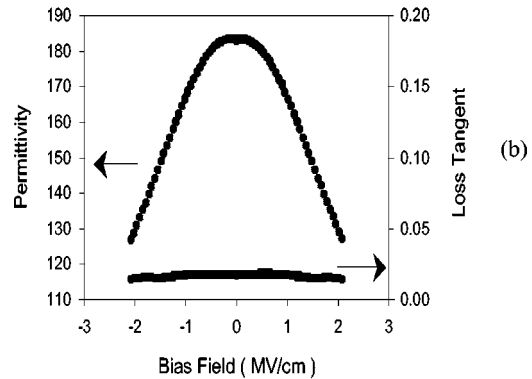
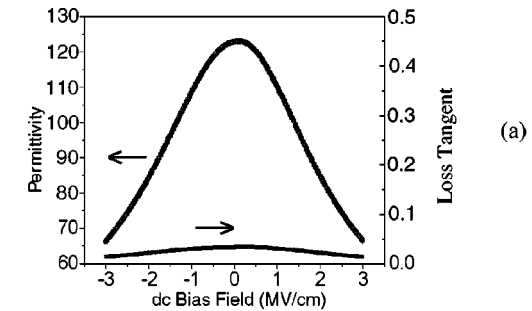


FIG. 10. Permittivity and loss tangent of (a) $\text{Bi}_{1.5}\text{Zn}_{1.0}\text{Nb}_{1.5}\text{O}_7$, (b) $\text{Bi}_{1.5}\text{Zn}_{0.5}\text{Nb}_{1.5}\text{O}_{6.5}$, and (c) $\text{Bi}_2\text{Zn}_{2/3}\text{Nb}_{4/3}\text{O}_7$ as a function of applied dc field, measured at 10 kHz and 0.03 V ac at 77 K.

TABLE II. Summary of dielectric properties in BZN films.

	Firing temperature (°C)	ϵ_r	Maximum tunability	Structure
$\text{Bi}_{1.5}\text{Zn}_{0.5}\text{Nb}_{1.5}\text{O}_{6.5}$	600	180	26% at 1.8 MV/cm	Cubic pyrochlore
$\text{Bi}_{1.5}\text{Zn}_{1.0}\text{Nb}_{1.5}\text{O}_7$	750	150	45% at 3 MV/cm	Cubic pyrochlore
$\text{Bi}_2\text{Zn}_{2/3}\text{Nb}_{4/3}\text{O}_7$	750	80	20% at 4 MV/cm	Zirconolite

and is in marked contrast to the substantial temperature dependence observed in many paraelectric compositions.

The major source of the ionic polarizability in the Bi pyrochlores with cubic symmetry come from the O'-Bi-O' bonds, as discussed by Kamba *et al.* and Nino *et al.*^{15,16} The lower frequency dipolar contributions are not fully understood, but the structure refinement by Levin *et al.* suggested the structure has a large potential for site disorder.¹² The random fields and their interaction between these disordered sites are believed to be the major sources of the polarizability in the lower frequency range. One possible cause of the tunability is that large fields (>1 MV/cm) applied to the thin films effectively clamp out this source of the polarizability. If this is so, then it would suggest that the maximum tunability will be on the order of 50% for the $\text{Bi}_{1.5}\text{Zn}_{1.0}\text{Nb}_{1.5}\text{O}_7$ composition.

It is possible to define a dielectric tunability figure of merit (FOM) as

$$\text{FOM} = Q \times \Delta\epsilon/\epsilon \times 100\%, \quad (2)$$

where Q is the quality factor at zero field, and $\Delta\epsilon/\epsilon$ is the field-induced change in permittivity relative to zero field permittivity, or the tunability. For the experiments performed here, a field of 1.8 MV/cm was used to induce a 30% tunability in $\text{Bi}_{1.5}\text{Zn}_{1.0}\text{Nb}_{1.5}\text{O}_7$, and has a FOM of 5900%. At 77 K, the tunability is 45%, but at this temperature, there is an increase in loss associated with the relaxation, which combine to reduce the FOM to 3400%. Similarly, the $\text{Bi}_{1.5}\text{Zn}_{0.5}\text{Nb}_{1.5}\text{O}_{6.5}$ films at 77 K have a tunability of 26% and a FOM of 1800%.

In contrast, the $\text{Bi}_2\text{Zn}_{2/3}\text{Nb}_{4/3}\text{O}_7$ zirconolite phase showed an unusual field dependence to the permittivity for high fields (≥ 700 kV/cm). As shown in Fig. 10(c), at 2 MV/cm there is a maximum in the permittivity; for fields greater than this, there is a rapid decrease in the permittivity to fields of 4 MV/cm. Films exposed to still higher fields were subject to dielectric breakdown. The increase in relative permittivity appears to be indicative of a field-induced phase transition. However, given the modest change in permittivity and the limited hysteresis observed on reversing the field, it is likely that the source of the tunability is a subtle change in the structure. One possible scenario that would be consistent with the observations is the ordering of the Zn cations within partially occupied, disordered sites in the hexagonal tungsten bronze layer of the structure as described by Levin *et al.*¹¹ This, though, requires direct proof and is not within the scope of this study.

For the measurements taken at 77 K and at 4 MV/cm, a maximum tunability of 20% can be induced, yielding a FOM

of 6100%. Unlike the cubic compositions, in $\text{Bi}_2\text{Zn}_{2/3}\text{Nb}_{4/3}\text{O}_7$ the figure of merit would likely be retained into the microwave frequency range.

IV. SUMMARY AND CONCLUSIONS

Three compositions in the Bi_2O_3 -ZnO- Nb_2O_5 system, $\text{Bi}_{1.5}\text{Zn}_{1.0}\text{Nb}_{1.5}\text{O}_7$, $\text{Bi}_{1.5}\text{Zn}_{0.5}\text{Nb}_{1.5}\text{O}_{6.5}$, and $\text{Bi}_2\text{Zn}_{2/3}\text{Nb}_{4/3}\text{O}_7$, were investigated in thin film form prepared by metalorganic decomposition methods. The $\text{Bi}_{1.5}\text{Zn}_{0.5}\text{Nb}_{1.5}\text{O}_{6.5}$ composition appears to be a previously unknown low temperature compound with a cubic pyrochlore structure, a permittivity of 180, low loss tangents, and a suppressed low temperature relaxation. This phase may undergo a peritectoid decomposition at 700 °C to a mixture of a cubic pyrochlore and BiNbO_4 . A summary of the important dielectric properties is given in Table II. The relaxation behavior in $\text{Bi}_{1.5}\text{Zn}_{0.5}\text{Nb}_{1.5}\text{O}_{6.5}$ and $\text{Bi}_{1.5}\text{Zn}_{1.0}\text{Nb}_{1.5}\text{O}_7$ follows an Arrhenius temperature dependence, with preexponentials in the ionic vibration range and activation energies of 0.13 and 0.11 eV, respectively. The high field dielectric properties are also similar for these two compositions, with a systematic decrease in the dielectric permittivity with increasing field strength. The same fractional tunability is available over at least a 200 °C temperature range. The field dependence on the dielectric permittivity in the zirconolite-structured $\text{Bi}_2\text{Zn}_{2/3}\text{Nb}_{4/3}\text{O}_7$ thin films shows an unusual field induced transition at high field ~ 2 MV/cm, which might be attributed to a field-forced ordering of the Zn atoms.

ACKNOWLEDGMENTS

We wish to acknowledge financial support from TDK Corporation and Intel Corporation during this project. We also wish to thank J. Aller for preparation of this manuscript.

¹O. Nakagawara, Y. Toyota, M. Kobayashi, Y. Yoshino, H. Tabata, T. Kawai, and Y. Katayama, *J. Appl. Phys.* **80**, 388 (1996).

²P. C. Joshi and S. B. Desu, *Appl. Phys. Lett.* **73**, 1080 (1998).

³P. C. Joshi, S. Stowell, and S. B. Desu, *Appl. Phys. Lett.* **71**, 1341 (1997).

⁴K. M. A. Salam, H. Fukuda, and S. Nomura, *J. Appl. Phys.* **93**, 1169 (2003).

⁵M. Klee, R. Kiewitt, W. Brand, P. Loebel, P. Lok, and F. Van Straten, *Integr. Ferroelectr.* **36**, 201 (2001).

⁶A. B. Catalan, J. V. Mantese, A. L. Micheli, N. W. Schubring, and R. J. Poisson, *J. Appl. Phys.* **76**, 2541 (1994).

⁷W. Ren, S. Trolier-McKinstry, C. A. Randall, and T. R. Shrout, *J. Appl. Phys.* **89**, 767 (2001).

⁸H. Funakubo (private communication).

⁹X. Wang, H. Want, and X. Yao, *J. Am. Ceram. Soc.* **80**, 2745 (1997).

- ¹⁰M. Valant and P. Davies, *J. Am. Ceram. Soc.* **83**, 147 (2000).
- ¹¹I. Levin, T. G. Amos, J. C. Nino, T. A. Vanderah, I. M. Reaney, C. A. Randall, and M. T. Lanagan, *Mater. Res. Bull.* **17**, 1406 (2002).
- ¹²I. Levin, T. G. Amos, J. C. Nino, T. A. Vanderah, C. A. Randall, and M. T. Lanagan, *J. Solid State Chem.* **168**, 69 (2002).
- ¹³J. C. Nino, M. T. Lanagan, and C. A. Randall, *J. Appl. Phys.* **89**, 4512 (2001).
- ¹⁴J. C. Nino, M. T. Lanagan, and C. A. Randall, *J. Mater. Res.* **16**, 1460 (2001).
- ¹⁵S. Kamba, V. Porokhonsky, A. Pashkin, V. Bortun, J. Petzelt, J. C. Nino, S. Troler-McKinstry, M. Lanagan, and C. A. Randall, *Phys. Rev. B* **66**, 054106 (2002).
- ¹⁶J. C. Nino, M. T. Lanagan, C. A. Randall, and S. Kamba, *Appl. Phys. Lett.* **81**, 4404 (2002).
- ¹⁷Y. P. Hong, S. Ha, H. Y. Lee, Y.-C. Lee, K. H. Ko, D. W. Hwang, H. B. Hong, and K. S. Hong, *Thin Solid Films* **419**, 183 (2002).
- ¹⁸G. W. Dietz, M. Schumacher, R. Waser, S. K. Streiffer, C. Basceri, and A. I. Kingon, *J. Appl. Phys.* **82**, 2359 (1997).
- ¹⁹D. Cann, C. A. Randall, and T. R. Shrout, *Solid State Commun.* **100**, 529 (1996).
- ²⁰M. F. Yan, H. C. Ling, and W. W. Rhode, *J. Am. Ceram. Soc.* **73**, 1106 (1995).
- ²¹D. Liu, Y. Liu, S. Huang, and X. Yao, *J. Am. Ceram. Soc.* **76**, 2129 (1993).